IEEE Access
Multidisciplinary | Rapid Review | Open Access Journal

Received October 30, 2017, accepted January 8, 2018, date of publication January 12, 2018, date of current version February 28, 2018.

Digital Object Identifier 10.1109/ACCESS.2018.2792400

Performance Modeling of LTP-HARQ Schemes Over OSTBC-MIMO Channels for Hybrid Satellite Terrestrial Networks

JIAN JIAO, (Member, IEEE), YOUJUN HU, QINYU ZHANG, (Senior Member, IEEE), AND SHAOHUA WU, (Member, IEEE)

Communication Engineering Research Center, Harbin Institute of Technology, Shenzhen, Guangdong 518055, China

Corresponding author: Shaohua Wu (hitwush@hit.edu.cn)

This work was supported in part by the National Natural Sciences Foundation of China under Grant 61771158, Grant 61525103, and Grant 61371102, in part by the Natural Scientific Research Innovation Foundation, Harbin Institute of Technology under Grant HIT NSRIF 2017051, and in part by the Shenzhen Basic Research Program under Grant JCYJ20160328163327348 and Grant JCYJ20150930150304185.

ABSTRACT Recently, with the development of Ka-band high throughput satellites and hybrid satellite-terrestrial networks, distributed/virtual multiple-input multiple-output (MIMO) technology over satellites have attracted considerable research interest. In this paper, a novel performance analysis framework is proposed for MIMO with orthogonal space-time block coding under Licklider transmission protocol (LTP) for emerging hybrid satellite terrestrial networks, where we derive the closed-form expressions of the mean number of transmission rounds by using Laplace transform for reliable data delivery in automatic repeat request (ARQ) and hybrid-ARQ schemes. Furthermore, we obtain the throughput expressions and unit information energy for lossless- and truncated-(H)ARQ schemes, and the maximum throughput and minimum unit information energy value on information rate. We also investigate the LTP file delivery time over Rayleigh and Rician fading channels. Simulations results are provided to demonstrate the validity of our theoretical results and show the effect of antenna number on the system performance.

INDEX TERMS Hybrid satellite terrestrial networks, OSTBC-MIMO system, HARQ, LTP, fading channels.

I. INTRODUCTION

A global coverage of hybrid satellite-terrestrial networks (HSTNs) will be one of the important infrastructures of fifth generation (5G) systems, and will enable a ''terabit data rate'' broadband wireless access capacity and offer the access availability of ''anywhere and anytime'' [1], to support emerging communications services, such as broadband broadcasting, disaster relief, air transport and ocean-going voyages [2].

Recently, delay/disruption tolerant networking (DTN) Licklider transmission protocol (LTP) has been developed to support space communications, which are different from terrestrial networks in terms of long signal propagation delay, high data corruption rates, and asymmetric channel rates [3]. LTP discards the three-times handshaking procedure and adopt the Negative Acknowledgment(NACK)-based feedback mechanism [4], which can mitigate the limitations of long distance and high interruption probability in the satellite-ground or inter-satellite links for HSTNs. Moreover, the throughput optimization for LTP with respect to the data rate over Ka-band channel was examined in [5].

On the other hand, multiple-input multiple-output (MIMO) technology for Ka-band millimeter-wave (mmWave) high-throughput satellites (HTS) has received a great deal of interests. The MIMO technology with orthogonal space-time block coding (OSTBC) have become key communication components to enhance the power and/or the spectral efficiency [6], [7]. Therefore, the goal of this paper is to develop a LTP-HARQ scheme over an OSTBC-MIMO block fading Additive Gauss White Noise (AWGN) channel for HSTNs.

A. RELATED WORKS AND MOTIVATION

The operations of DTN rely on the bundle protocol(BP) to form a store-and-forward overlay network, where BP handles data message transmission and reception by invoking the services of an underlying convergence layer adapter (CLA). Transmission control protocol-(TCP-) CLA, user datagram protocol- (UDP-) CLA and LTP-CLA are the most broadly

supported CLAs under BP [8]. In [9], the experimental evaluation of BP delay performance in cislunar communication scenario was presented, and the performance comparison between TCP-CLA and LTP-CLA was given. Reference [10] proposed a file delivery time performance model of the LTP-based DTN data transmission scheme. Reference [11] concentrated on the dynamic memory for using LTP in a dual-hop deep-space communication infrastructure. Reference [12] provided the analysis of throughput performance, quantify buffering, and file delivery time in deep space communication scenarios.

The above literature focused on the performance of the original ARQ mechanism in LTP, which limited the efficiency of LTP in the challenging communication conditions. Hence, to increase the transmission efficiency as well as the throughput of the HSTN system, we introduce the HARQ transmission mechanism into LTP.

First, appropriate metrics to evaluate the performance of ARQ and HARQ mechanisms in HSTNs need to be provided. The expected number M of the transmission rounds of HARQ and the throughput expression over the Gaussian channel was given in [13]: $M = \sum_{k=1}^{\infty} Q_k$, where Q_k denotes the decoding failure probability after k-th transmission. In [14], the throughput and outage probability (OP) performance of ARQ were obtained over quasi-static fading channels. Reference [15] derived the throughput for network-coded HARQ over Rayleigh fading channels. Further, the throughput of wireless multicast systems was analyzed and the closed-form approximation for the dynamic rate in HARQ with repetition redundancy (RR) was derived in [16]. Hence, our performance evaluation models for ARQ and HARQ can be found with the help in aforementioned works.

However, the lossless (H)ARQ may cause waste of energy under the HSTN channel conditions, due to the lack of instant channel state information and unlimited transmission rounds. Reference [17] considered the maximum throughput problem, and proposed an optimization rate-adaptation and rate-allocation scheme by using dynamic programming framework for the truncated HARQ. The performance of OP under adaptive power allocation scheme for the truncated HARQ over the Nakagami-m block fading channels was studied in [18]. Moreover, a closed form expression for the mean number of transmission rounds M and throughput T in the lossless HARQ and truncated HARQ over Gaussian block fading channels were presented in [7], by using Laplace transform to simplify the probability density function (pdf) of power gain distribution, which solved the difficulty of infinite accumulation of Q_k. Further, Larsson [19] proposed a matrix exponential (ME) distribution to model the mean number of transmission rounds M and throughput T over Rayleigh fading channel.

In addition, the energy consumption of our LTP-HARQ mechanism is one of the key parameters in HTSN communications. In [20], the energy efficiency of non-collaborative HARQ and collaborative HARQ in terms of the transmitting and receiving electronic circuitry was studied. In [21], the energy efficiency of HARQ for delivering one bit data without error was studied, the code rate of the error correcting code is optimized, and a model of the HARQ retransmission scheme on the average energy requirement was established. Reference [22] used the Markov decision process framework to find an optimal adaptive policy of energy efficiency for the lossless HARQ and truncated HARQ protocols, where the adaptation of the code blocklength can provide notable gains than the power adaptation and conventional HARQ. The energy efficiency and spectral efficiency of HARQ-RR are optimized and compromised over Rayleigh fading channel in [23]. In [24], the energy efficiency optimization method of HARQ-RR based on low-parity parity check (LDPC) codes was studied. These documents established the energy consumption model of the HARQ and studied the optimization of the energy and spectral efficiency, however, the energy optimization for the HARQ mechanism with respect to the signal noise ratio (SNR) or the data rate is still an open problem.

Thus, in this paper, we build a mathematical model to describe the mean number of transmission rounds, the throughput and energy consumption of LTP-(H)ARQ over OSTBC-MIMO system. To the best of our knowledge, this is the first work to analyze the LTP over fading channels for HSTN. Further, few studies on the energy consumption of LTP and lack of discussion of the optimal value of energy consumption in terms of SNR.

B. CONTRIBUTIONS

The main contributions of this paper are outlined as follows:

- We propose a LTP-HARQ protocol based on OSTBC-MIMO system for distributed MIMO HTS communication scenarios in HTSNs. We derive the closed-form expressions of the mean number of transmission rounds (15) of our proposed LTP-HARQ, and the theoretical solution of transmission delay is also obtained (7).
- By using the Laplace transform approach, we derive the theoretical solution of performance metrics for different transmission mechanisms over Rician fading channel, including lossless HARQ (15), (16), truncated HARQ (22), (23), and ARQ (27), (28). Also, we give the reference for Nakagami-m fading channels (48), (51).
- We analysis the performance metrics of the unit information energy for the LTP-HARQ with OSTBC-MIMO system over Rayleigh and Rician fading channel, and demonstrate that there exists a SNR value S can minimize the transmission energy consumption per unit information (Theorem 1 and Theorem 2). Also, we prove that there exist information transmission rate R which can maximize the throughput (Theorem 3) and minimize the unit information energy (Theorem 4).

C. OUTLINE

The reminder of this paper is organized as follows. In Section II, we present the system model. The closed-form

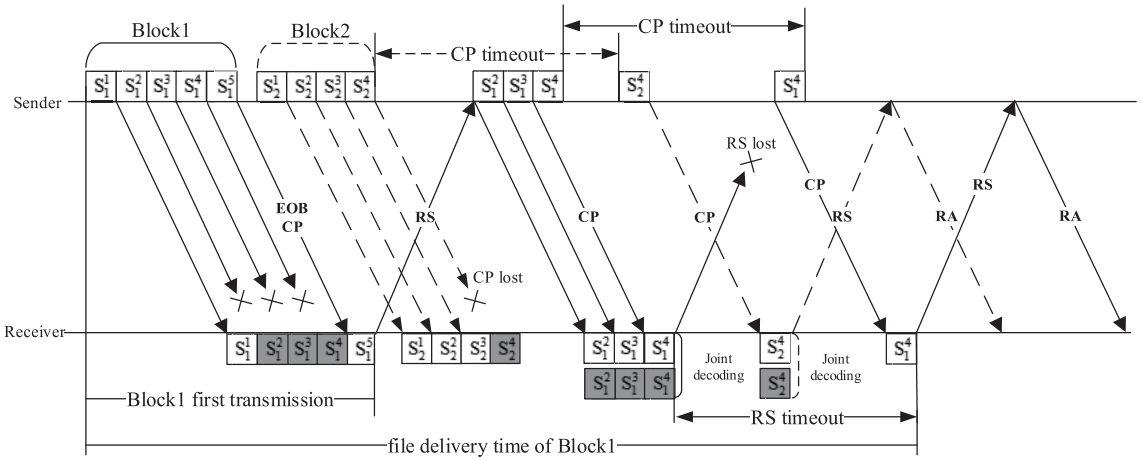

FIGURE 1. The proposed LTP-HARQ transmission scheme.

expressions of the mean number of transmission rounds and unit information energy consumption for reliable data delivery in the LTP-(H)ARQ schemes are derived in Section III, and the throughput and file delivery time for the LTP-(H)ARQ schemes are also analyzed over Rayleigh and Rician fading channels. In Section IV, we present the numerical and simulation results, and we analysis the optimization value accordingly. Finally, we conclude the paper in Section V.

II. SYSTEM MODEL

In this section, we present an analytical model to characterize the operation and performance of our LTP-HARQ scheme in HTSNs. The space nodes in HTSNs have features of sparse and dynamic topology, long and variant propagation delay, lossy data links and highly asymmetric channel rates. Based on the LTP applied to the challenging space communication environment, the collaboration between distributed MIMO HTS and HTSNs node can improve the effectiveness and reliability of satellite-station link.

The OSTBC-MIMO system helps the HTSN system to combat the channel fading and achieve the diversity gain, and we introduce the HARQ mechanism instead of ARQ mechanism into LTP, which could significantly improve the transmission efficiency. The proposed LTP-HARQ transmission scheme is shown in Fig. 1, where the receiver can store the undecoded/corrupted segments in its decoder buffer and perform a joint decoding with the future retransmission segments, which can effectively enhance the throughput over OSTBC-MIMO channels for HSTNs.

In LTP transmission, the sender transmits the data blocks in a continuously series manner, each block is fragmented into the LTP data segments. The LTP data segments are then recognized by two parts: a ''red-part'', whose delivery must be assured by acknowledgment and retransmission, and a ''green-part'', whose delivery is attempted, but not assured. According to the report segment (RS) of the LTP data segments and to maximize the underlying link service, each segment is annotated with both of its displacement and length from the start of the block. The last segment of each LTP data block, which contains only red data, is flagged as a checkpoint (CP) to elicit a reception report and also as an end of block (EOB) to indicate the total block length, and the sender use a timer to ensure the reliable transmission of CP as shown in Fig. 1. RS indicates the cumulative reception status of the block, and the receiver also use a timer to ensure the reliable transmission of RS. Report-Acknowledge (RA) segment indicates the end of transmission, and the red segments which contain transmission data are important elements for the LTP transmission process [25]. The detailed process of red segments transmission, referring to Fig. 1, is shown as follows:

The LTP transmission starts upon the upper layer protocol request. In Fig. 1, Block1 is divided into 5 data segments (four regular segments and last segment is flagged as CP) will be transmitted in the first transmission round. The next block (e.g., Block2) is in query. If the sender finish the first transmission round of Block1, the CP timer is on. The RS timer in the receiver would be started if the retransmission of the red data segment is needed. The receiver feedback a RS after received CP, which declaim that three segments are failed to decode, and the three failure segments will be stored in the receiver's buffer and wait for the future joint decoding chance in our LTP-HARQ mechanism. The sender will resent the failure segments indicated by the RS instantly after send an ongoing transmission of data block. Unlike the LTP-ARQ mechanism, our LTP-HARQ receiver can use the previously stored undecoded segments to joint decode the retransmitted segments. If a RS indicates all of the segments are correctly received, the sender then issue a RA and finish the transmission of Block1.

Moreover, we assume each segment is an input data of the OSTBC-MIMO system, transmitted by N_t antennas Node1 and received by N_r antennas Node2, as shown

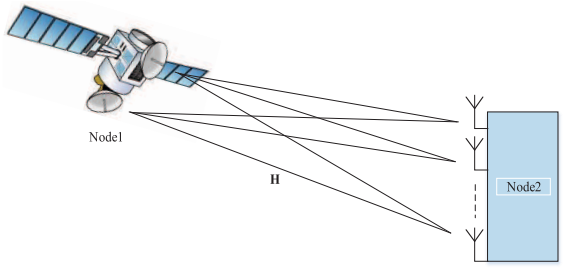

FIGURE 2. The diagram of distributed MIMO satellite communication.

in Fig. 2. Let r denotes the OSTBC code rate. The diversity order of the maximum ratio combing (MRC) for the OSTBC-MIMO system is calculated by $N = N_t \times N_r$. We consider the HARQ mechanism of the OSTBC-MIMO system communication over a block fading AWGN channel, and the received signal is

$$Y = \sqrt{S}HX + W, \tag{1}$$

where Y, H, X, W are the complex matrices with dimension of $C^{N_r \times N_x}$, $C^{N_r \times N_t}$, $C^{N_t \times N_x}$, $C^{N_r \times N_x}$, respectively, and H_{ij} denotes the power gain from j-th transmitter antenna to i-th receiver antenna. Assume that H_{ij} is independent identically distributed (i.i.d.), and $H_{ij} \sim CN(0, 1)$. The AWGN channel noise follows the complex Gaussian distribution, $W_{ij} \sim CN(0, 1)$. Let S denotes the average SNR of the single-input single-output (SISO) channel, and the average noise power is set as 1. Moreover, H_{ij} is quasi-static, and the multiple complex Gaussian signals are superimposed on the receiver due to the diversity, and the channel gain follows the χ^2 distribution with the freedom degree is $2N$.

The performance of state-of-the-art Turbo codes [26], [27] and LDPC codes [28] have been proved to approach the Shannon limit, which can be used to encode the LTP data segment to enhance the error correcting capacity. Therefore, we mainly consider the following three transmission mechanism in the LTP transmission:

1) ARQ: If the receiver fails to decode the received segments, the received coded data segments is discarded and a RS is feedback from the receiver till successful reception. Every retransmission segment contains the same information and parity bits.
2) Lossless HARQ: If the received data fails to be decoded, incorrectly received coded data segment is stored at the receiver rather than discarded, and when the retransmission segment is received, these two segments are joint decoding. The retransmission and joint decoding will continue till all the segments are successful recovered.
3) Truncated HARQ: The decoding and retransmission process is the same as the lossless HARQ, except that there exist an upper limit of transmission rounds C for the truncated HARQ. If the data is not correctly decoded after $C-1$ retransmission rounds, it will be dropped.

The performance analysis of ARQ, lossless HARQ-RR, and truncated HARQ-RR in LTP are studied in this paper. To facilitate the derivation, we define the relevant mathematical functions and symbols as follows: The Laplace transform $F(s)$ of the function $f(x)$, $F(s) = L\{f(x)\}_s = \int_0^\infty e^{-sx} f(x)dx$ and the inverse Laplace transform $f(x) = L^{-1}\{F(s)\}_x = \frac{1}{2\pi i}\lim_{T\to\infty}\int_{\tau-iT}^{\tau+iT} e^{sx}F(s)ds$. $\Gamma_r(\alpha, x) = \frac{1}{\Gamma(\alpha)}\int_x^\infty t^{\alpha-1}e^{-t}dt$ is the regularized upper incomplete gamma function and $\gamma_r(\alpha, x) = \frac{1}{\Gamma(\alpha)}\int_0^x t^{\alpha-1}e^{-t}dt$ is the regularized lower incomplete gamma function, where $\gamma_r(\alpha, x) = 1 - \Gamma_r(\alpha, x)$, if α is an integer, $\Gamma(\alpha) = (\alpha-1)!$.

III. PERFORMANCE ANALYSIS

A. PERFORMANCE METRICS

1) THE MEAN NUMBER OF TRANSMISSION ROUNDS

First, we investigate the mean number of transmission rounds M_{LTP} of a data block in the LTP-HARQ protocol, i.e., M_{LTP} is the number of transmission rounds for all of the segments in one data block are delivered to the receiver. M_{LTP} can greatly affect many other performance metrics such as file delivery time, throughput and energy consumption. Let M denotes the mean number of transmission rounds for one segment. In the conventional LTP-ARQ mechanism, M is given by $M = 1/(1-Q)$, where Q is the decoding failure probability of the segment, which is determined by bit error rate (BER) and the length of the segment. Let Num denotes the number of segments in one data block, then M_{LTP} is given by [29]

$$\begin{aligned} M_{LTP} &= \sum_{m=1}^{\infty}[1-(1-Q^{m-1})^{Num}], \\ &= 1+\sum_{m=2}^{\infty}[1-(1-Q^{m-1})^{Num}], \end{aligned} \tag{2}$$

where Q has the different expressions corresponding to the different fading channels and transmission mechanisms.

Moreover, define R as the normalized data rate (bit/Hz/s), the mean number of transmission rounds (including the first transmission effort and retransmission efforts) for one segment is denoted by

$$M = \sum_{k=1}^{\infty} kP_k = \sum_{k=1}^{\infty} k(Q_{k-1} - Q_k) = \sum_{k=0}^{\infty} Q_k, \tag{3}$$

where P_k and Q_k denote the successful decoding probability and the decoding failure probability of the k-th transmission round, respectively, and $Q_0 = 1$. In the k-th HARQ transmission round, the previous $k-1$ rounds undecoded data will be used to joint decoding with the k-th transmission segment. Let Q_{k-1} denote the decoding failure probability of $(k-1)$-th transmission round, then P_k and Q_k satisfy the $Q_{k-1} = P_k + Q_k$. The decoding failure probability Q_k (i.e., the OP from the perspective of information theory) can be denoted by

$$Q_k = P(i_k \le R), \tag{4}$$

where $i_k \leq R$ means that the accumulated mutual information realization after k-th transmission for a segment does not satisfy the decoding threshold. When the data decoding fails in ARQ mechanism, the error data is discarded at the receiver, and the k-th successful decoding probability have no mutual information accumulation gain from the previous $k-1$ transmission rounds, i.e., $i_k = i_{k-1}$. However, for the HARQ-RR mechanism, the receiver uses MRC to combine the retransmitted bits with the previous stored bits, and the mutual information gain is obtained by adding the same multiple transmitted bits which increased the SNR. The accumulated mutual information is denoted by $i_k^{RR} = \ln(1 + S\sum_{u=1}^{k} z_u)$, where the random variable z_k denotes the channel power gain for the k-th transmission, and its pdf $f_Z(z)$ follows different distributions over different fading channels. We can further rewrite (4) for the SISO channel as follows

$$Q_k = P\{i_k \leq R\} = P(\sum_{u=1}^{k} z_u \leq \Theta) = \int_0^{\Theta} f_Z{}^{\otimes(k)}(z)dz, \quad (5)$$

where we define the decoding threshold $\Theta^{RR} = \left(e^R - 1\right)/S$. z_u is i.i.d., $z \sim f_Z(z)$, and $f_Z{}^{\otimes(k)}$ is the k-fold convolution. According to the different distribution of $f_Z(z)$, we can obtain the Q_k for the different fading channels.

2) THROUGHPUT AND TRANSMISSION DELAY OF LTP-HARQ

Based on the mean number of transmission rounds for a data block, we have the throughput definition [30] without considering the influence of propagation delay as follows

$$T = R/M, \quad (6)$$

where we define the normalized-bandwidth information rate per channel transmission is $R = L_{seg}/BD_{seg}$, which means under the bandwidth B, L_{seg} nats information are transmitted in slot D_{seg}. In the LTP-HARQ transmission process, D_{seg} denotes the average process time per segment at the sender. Therefore, the transmission delay for a single block in a single hop scenario is given by the following according to [10]:

$$\begin{aligned} D_{block} &= D_{trans} + D_{prop\_total} + D_{CP\_total} + D_{RS\_total}, \\ &= Num \times D_{seg} \times M + (2M_{LTP} - 1)\, D_{prop} \\ &\quad + (M-1)(D_{CP} + D_{CP\_timer})(M_{LTP} - 1) \\ &\quad + (M-1)(D_{RS} + D_{RS\_timer})(M_{LTP} - 1). \end{aligned} \quad (7)$$

The file delivery time for a single block D_{block} includes the average segments transmission time D_{trans}, propagation delay of entire block D_{prop_total}, the timeout value of CP segment timer is D_{CP_total}, and the timeout value of RS segment timer is D_{RS_total}. The total number of segments that need to be transmitted to ensure successful delivery of the entire block can be rewritten as $Num = L_{block}/L_{seg}$, where L_{block} is the block size and L_{seg} is the segment length. The total propagation time D_{prop_total} is the main delay in the long distance HSTN communication scenario. We set the timeout of CP segment timer as $D_{CP\_timer} = 2D_{prop} + D_{RS}$, and the timeout of RS segment timer $D_{RS\_timer} = 2\,D_{prop} + D_{CP}$ for the best transmission efficiency. Where we assume CP, RS and data segment have an identical length, and the transmitting slot for one segment can be set as $D_{CP} = D_{RS} = D_{seg}$ [10].

3) UNIT INFORMATION ENERGY

We now have the expressions of general file delivery time and the throughput based on the mean number of transmission rounds. To sketch a general framework for the LTP-HARQ mechanism, we investigate the energy consumption, and define the unit information energy as the energy consumption by successfully transmitting one unit information. The unit can be expressed in bit or nat. For the integral operation convenience in this paper, we use nat and express T and R in [nat/Hz/s] in the equations. The total energy per successfully transferred nat or the unit information energy is denoted as in [21]

$$E_b = E/N_b = E_t + E_r, \quad (8)$$

where E represents the total energy consumed by transmitting the segments and N_b denotes the segment size. The energy consumption mainly comes from two parts: transmitter and receiver. E_t and E_r mean the energy consumed per goodbit (one successful data bit) at the transmitter and the receiver. Actually, E_t is the unit information energy at transmitter and E_r is similar. Further, we can rewrite (8) as

$$E_b = A_0 S D_{seg} M/L_{seg} + M E_d, \quad (9)$$

The data segment with size L_{seg} is transmitted by M transmission rounds in slot D_{seg} and A_0 is the coefficient. E_d denotes the unit information energy by the electronic components and decoding at B. By using the substitution $R = L_{seg}/BD_{seg}$ and setting $A_0 = 1$ (the detailed deduction is shown in the Appendix A), we arrive at

$$E_b = \frac{S}{BT} + M E_{dec}. \quad (10)$$

The normalized-bandwidth information energy E_{dec} is related to the decoding and electronic components, which is differen in ARQ, lossless HARQ-RR and truncated HARQ-RR, and denote as E_{dec}^{ARQ}, E_{dec}^{RR}, and E_{dec}^{C}, respectively. Based on the LTP performance metrics such as transmission delay, the mean number of transmission rounds, throughput, and unit information energy, we then provide the detailed derivations and expressions. At the same time, considering the influence factors on the HSTN line of sight (LOS) channel gain, such as the weather condition, atmospheric absorption, and solar scintillation, etc, the Rician fading channel will be taken into account. Also, we will give the related results over Rayleigh fading channel as comparison.

B. PERFORMANCE ANALYSIS OF LOSSLESS-HARQ

Consider the lossless HARQ-RR in the OSTBC-MIMO system with N order diversity. In this case, the signals are transmitted by uncorrelated antennas and the MIMO channel is

degenerated into an effective SISO channel [31]. The segment decoding failure probability of k-th transmission round can be rewritten as

$$\begin{aligned} Q_k &= P\left\{ r\ln(1+S/(rN_t)\sum_{u=1}^{k} z_u) \le R \right\}, \\ &= P(\sum_{u=1}^{k} z_u \le \Theta) = \int_0^{\Theta} f_Z{}^{\otimes(k)}(z)dz, \end{aligned} \tag{11}$$

where $\Theta = (\exp(R/r)-1)/\widetilde{S}$ means the decoding threshold, and $\widetilde{S} = S/(rN_t)$ is so-called effective SNR. r is the code rate. z_u represents the channel power gain, and its pdf over Rician fading channel is shown as follows

$$f_Z(z) = \sum_{i=0}^{\infty} \frac{\exp(-KN)(KN)^i}{\Gamma(i+1)} \frac{z^{N-1+i}\exp(-z)}{\Gamma(N+i)}. \tag{12}$$

And the Laplace Transform is expressed as

$$F(s) = \sum_{i=0}^{\infty} \frac{\exp(-KN)(KN)^i}{\Gamma(i+1)} (1+s)^{-(N+i)}. \tag{13}$$

The decoding failure probability of k-th transmission segment over Rician fading channel can be expressed as

$$Q_k = e^{-(kKN)} \sum_{i=0}^{\infty} \frac{(kKN)^i}{\Gamma(i+1)} \gamma_r(kN+i,\Theta). \tag{14}$$

The derivation of (12), (13), (14) are shown in Appendix B. Moreover, we can get the mean number of transmission rounds of HARQ-RR over Rician fading channel by the definition (3) and rewrite as follows

$$\begin{aligned} M_{Ric}^{RR} &= \sum_{k=0}^{\infty} Q_k, \\ &= \sum_{k=0}^{\infty} \exp(-kKN) \sum_{i=0}^{\infty} \frac{(kKN)^i}{\Gamma(i+1)} \gamma_r(kN+i,\Theta). \end{aligned} \tag{15}$$

Then, the throughput of HARQ-RR system over Rician fading channel is given as

$$T_{Ric}^{RR} = \frac{R}{\sum_{k=0}^{\infty} \exp(-kKN) \sum_{i=0}^{\infty} \frac{(kKN)^i}{\Gamma(i+1)} \gamma_r(kN+i,\Theta)}, \tag{16}$$

where K denotes the shape parameter of Rician fading, $K = D^2/2\sigma^2 = D^2$, which denotes the ratio of the power contributions by LOS path to the remaining multipaths.

The mmWave HTS fading channel could degenerate to Rayleigh fading channel under the rainy weathers. The mean number of transmission rounds and the throughput over Rayleigh fading are given by [7]

$$M_{Ray}^{RR} = \frac{N+1}{2N} + \frac{\Theta}{N} + \frac{1}{N} \sum_{n=1}^{N-1} \frac{\exp(-\Theta b_n)}{{b_n}^*}, \tag{17}$$

and

$$T_{Ray}^{RR} = \frac{2NR}{N+1+2\Theta+2\sum_{n=1}^{N-1} \exp(-\Theta b_n)/{b^*}_n}, \tag{18}$$

where $*$ denotes the complex conjugate, and $b_n = 1-a_n$, $a_n = \exp(i2\pi n/N)$ is the n-th root of unity. We can obtain the mean number of HARQ-RR transmission rounds for the block over Rician fading by combining (2) and (14) as follows

$$M_{LTP}^{RR\_Ric} = 1 + \sum_{m=2}^{\infty} [1 - (1 - \prod_{j=1}^{m-1} P_{seg}^{RR\_Ric}(m,N,\Theta))^{Num}], \tag{19}$$

where $P_{seg}^{RR\_Ric}(m,N,\Theta))^{Num} = Q_k$ can be obtained by (14). The mean number of LTP-HARQ transmission rounds over Rayleigh fading is

$$M_{LTP}^{RR\_Ray} = 1 + \sum_{m=2}^{\infty} [1 - (1 - \prod_{j=1}^{m-1} \gamma_r(mN,\Theta))^{Num}]. \tag{20}$$

By substituting (15), (19) or (17), (20) into (7), we can obtain the file delivery time over Rician and Rayleigh fading channels, respectively.

According to (10), (14), and (16), we can get the unit information energy under the OSTBC-MIMO system in LTP-HARQ mechanism as follows

$$E_b = \begin{cases} \dfrac{S}{BT_{Ric}^{RR}} + M_{Ric}^{RR} E_{dec}^{RR}, & \text{Rician fading,} \\ \dfrac{S}{BT_{Ray}^{RR}} + M_{Ray}^{RR} E_{dec}^{RR}, & \text{Rayleigh fading.} \end{cases} \tag{21}$$

Considering the lossless HARQ over Rayleigh or Rician fading channel, and combing the formula (16), (18), and (21), we have the following theorem by substituting the limit of unit information energy E_b.

Theorem 1: For the OSTBC-MIMO system with lossless HARQ transmission mechanism over Rayleigh or Rician fading channels, there is an appropriate value of SNR S, which makes the unit information energy cost lowest. Moreover, for the power amplifier sender, no matter how low the SNR is, the decoding can always success due to the infinite retransmission rounds.

Proof of Theorem 1: The proof is given in Appendix C.

Thus, we have obtained the mean number of transmission rounds, throughput, file delivery time and unit information energy for the lossless HARQ mechanism in LTP.

C. PERFORMANCE ANALYSIS OF TRUNCATED HARQ AND ARQ

Unlike the lossless HARQ, the mean number of transmission rounds of truncated HARQ has an upper limit C. When the transmission rounds reaches the upper limited C without successful decoding, the transmitter will drop the data segment and begin the next transmission. Therefore, the truncated

HARQ can not guarantee the full reliability of file delivery, but it can avoid the energy waste due to the unlimited retransmission rounds. By using (3) and (14), we obtain the mean number of transmission rounds of truncated HARQ over Rician fading as

$$M_{Ric}^{C} = \sum_{k=0}^{C-1} Q_k = \sum_{k=0}^{C-1} \exp(-kKN) \sum_{i=0}^{\infty} \frac{(kKN)^i}{\Gamma(i+1)} \gamma_r(kN+i,\Theta). \quad (22)$$

Thus, the throughput expression of the truncated HARQ is given as follows

$$T_{Ric}^{C} = \frac{R\left\{1-\exp(-CKN)\sum_{i=0}^{\infty}\frac{(CKN)^i}{\Gamma(i+1)}\gamma_r(CN+i,\Theta)\right\}}{\left\{\sum_{k=0}^{C-1}\exp(-CKN)\sum_{i=0}^{\infty}\frac{(kKN)^i}{\Gamma(i+1)}\gamma_r(kN+i,\Theta)\right\}}. \quad (23)$$

Similarly, we can obtain the expected number of transmissions rounds and the throughput expressions of truncated HARQ over Rayleigh fading channel as follows

$$M_{Ray}^{C} = 1 + \sum_{k=1}^{C-1} \gamma_r(Nk,\Theta), \quad (24)$$

and

$$T_{Ray}^{C} = \frac{R\Gamma_r(NC,\Theta)}{1+\sum_{k=1}^{C-1}\gamma_r(Nk,\Theta)}. \quad (25)$$

Because the truncated HARQ mechanism can not meet the reliability requirements of red data transmission in LTP, we only consider the mean number of transmission rounds, throughput, and energy consumption as a comparison to the lossless HARQ. The unit information energy can be expressed from (10) as follows

$$E_b = \begin{cases} \frac{S}{BT_{Ric}^{C}} + M_{Ric}^{C}E_{dec}^{C}, & \text{Rician fading,} \\ \frac{S}{BT_{Ray}^{C}} + M_{Ray}^{C}E_{dec}^{C}, & \text{Rayleigh fading.} \end{cases} \quad (26)$$

In the ARQ mechanism, the decoding failure probability does not help reducing the transmission rounds. The mean number of transmission rounds is $M^{ARQ} = 1/(1-Q_1)$ and throughput $T^{ARQ} = R(1-Q_1) = R(1-\int_0^{\Theta} f_Z(z)dz)$. Further, we can get the mean number of transmission rounds and throughput expressions of the ARQ mechanism over Rician and Rayleigh fading as follows

$$M_{Ric}^{ARQ} = \frac{1}{1-\sum_{i=0}^{\infty}\frac{\exp(-KN)(KN)^i}{\Gamma(i+1)}\gamma_r(N+i,\Theta)}, \quad (27)$$

$$T_{Ric}^{ARQ} = \left\{1-\sum_{i=0}^{\infty}\frac{\exp(-KN)(KN)^i\gamma_r(N+i,\Theta)}{\Gamma(i+1)}\right\}R, \quad (28)$$

$$M_{Ray}^{ARQ} = 1/\Gamma_r(N,\Theta), \quad (29)$$

$$T_{Ray}^{ARQ} = R\Gamma_r(N,\Theta), \quad (30)$$

where (27) and (28) represent the mean number of transmission rounds and throughput over Rician fading channels, respectively, where (29) and (30) are over Rayleigh fading channels.

We should notice the result that for truncated HARQ $C = 1$ and ARQ mechanisms, we have the same throughput expression $T_{Ric}^{C} = T_{Ric}^{ARQ}$ and $T_{Ray}^{C} = T_{Ray}^{ARQ}$ [7]. Then the unit information energy of the ARQ mechanism is given as follows

$$E_b = \begin{cases} \frac{S}{BT_{Ric}^{ARQ}} + M_{Ric}^{ARQ}E_{dec}^{ARQ}, & \text{Rician fading,} \\ \frac{S}{BT_{Ray}^{ARQ}} + M_{Ray}^{ARQ}E_{dec}^{ARQ}, & \text{Rayleigh fading.} \end{cases} \quad (31)$$

According to the energy consumption of the truncated HARQ and ARQ mechanisms, we can get the following theorem.

Theorem 2: For the OSTBC-MIMO system with truncated HARQ or ARQ transmission mechanism over the Rayleigh or Rician fading channels, there is an appropriate value of SNR S, which makes the unit information energy cost lowest. However, for power amplifier sender, truncated HARQ and ARQ can not guarantee the final decoding success due to the finite retransmission rounds.

Proof of Theorem 2: The proof is given in Appendix D.

Therefore, we have obtained the throughput, unit information energy and LTP file delivery time performance for lossless HARQ-RR, truncated HARQ and ARQ mechanism over Rician and Rayleigh fading channel under OSTBC-MIMO system with diversity N.

IV. SIMULATION RESULTS AND DISCUSSION

In this section, Monte Carlo simulations carries on the mean number of transmission rounds, and we evaluate the throughput, file delivery time and unit information energy performance for lossless HARQ, truncated HARQ and ARQ schemes under OSTBC-MIMO system over different fading channels.

First, we investigate the mean number of transmission rounds M for ARQ, lossless HARQ and truncated HARQ. To facilitate discussion, the diversity order under OSTBC-MIMO system is set as 1 and the channel is degraded into SISO channel. Consider a cislunar communication scenario [9], the information rate is $R = 2$ nats/Hz/s and other parameters are selected from Table 1.

According to (13), (15), (22), (24), (27), and (29), the simulation result is shown in Fig. 3. Obviously, the performance over Rician fading channel is better than Rayleigh fading channel in Fig. 3 due to the LOS affect. It is also worth noting that the mean number of transmission rounds for truncated HARQ is limited to C at the SNR value $S = 0$. If the SNR is limited to infinity, the retransmission for the data block is unnecessary. From the results of Monte Carlo simulation,

TABLE 1. Experimental parameters and configurations.

Experimental Factors	Settings/Values
Code rate of OSTBC	$r = 1$
Diversity order	N=1,2,3,4,where $N_t = 1$
Shape parameter	K=0.1
Upper limit of truncated HARQ	$C = 2$
Block size	$L_{block} = 244000bytes$
Segment size	$L_{seg} = 1400bytes$
One-way propagation delay	$T_{prop} = 1.2s$
CP or RS segment size	$L_{seg} = 1400bytes$
Channel bandwidth	B = 31.1 MHz

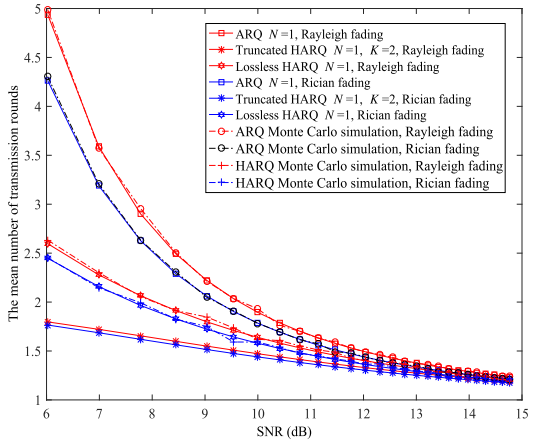

FIGURE 3. The mean number of transmission rounds of ARQ, truncated HARQ with C=2 and lossless HARQ over Rician and Rayleigh fading channel.

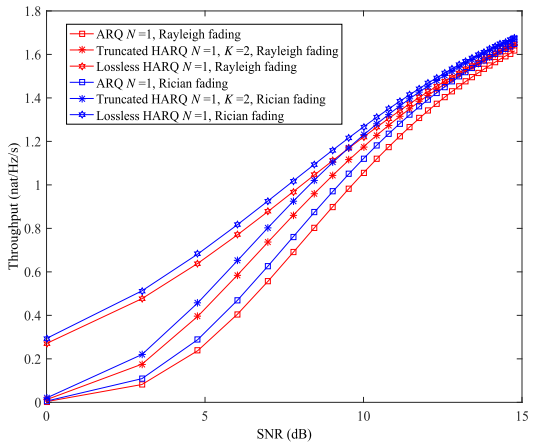

FIGURE 4. The throughput performance of ARQ, truncated HARQ with $C = 2$ and lossless HARQ over Rician and Rayleigh fading channel.

we find a good agreement between the experiment results and theoretical method curve. The other performance metrics, e.g., the throughput and unit information energy, are based on the mean number of transmission rounds.

By using (14), (16), (23), (25), (28), and (30), the throughput performance result is shown in Fig. 4. It is easy to find that the throughput is limited to 0 with SNR decreasing to 0, and it is limited to R with the SNR increasing to infinity.

The file delivery time under the OSTBC-MIMO system in LTP-HARQ protocol is shown in Fig. 5. Obviously, we can see that the file delivery time of the lossless HARQ has better performance compared to the original ARQ mechanism in LTP, especially in the low SNR value regime.

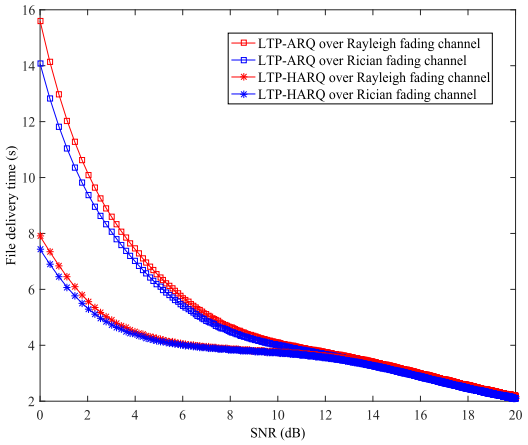

FIGURE 5. Comparison of file delivery time of LTP-HARQ and LTP ARQ over Rayleigh and Rician fading channel.

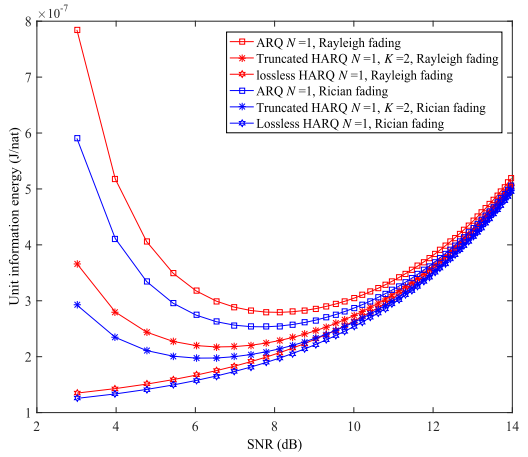

FIGURE 6. The unit information energy of ARQ, truncated HARQ with $C = 2$ and lossless HARQ over Rician and Rayleigh fading channel.

The energy consumption performance in the LTP-HARQ mechanism under OSTBC-MIMO system is shown in Fig. 6, which is also a graphic display of Theorem 1 and Theorem 2. For the lossless HARQ, truncated HARQ and ARQ mechanism, there exists a theoretical nadir of unit information energy with respect to SNR S, which can help us to find the optimal transmitting power. Then we give the energy consumption evaluation of power amplifier at the transmitter and obtain some useful conclusions in the next.

We mainly discuss the effect of the information rate R on the system performance. According to the derived throughput expressions (16) and (18) over Rician and Rayleigh fading channel, the impact of the information transmission rate on throughput is shown in Fig. 7. We can get the following observations: a) Throughput performance can be improved by increasing the diversity order; b) The throughput performance under OSTBC-MIMO system has a specific R which leads to the maximum throughput. Thus we can get Theorem 3.

Theorem 3: For the OSTBC-MIMO system over Rayleigh and Rician fading channels, there exists an information transmission rate R leads to the maximum throughput $T = T_{MAX}$.

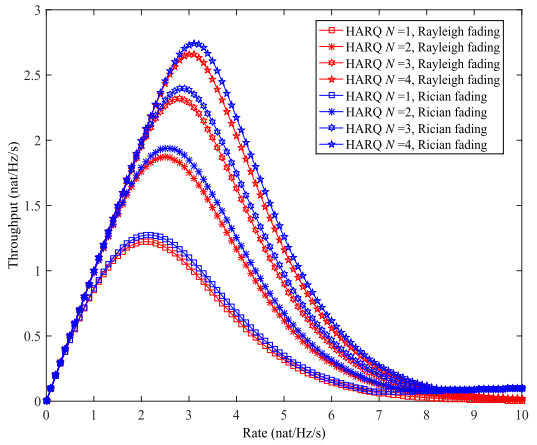

FIGURE 7. The effect of information transmission rate versus throughput.

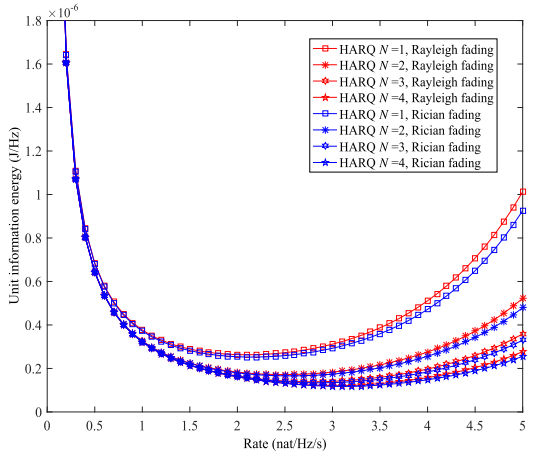

FIGURE 8. The effect of information rate R versus unit information energy.

Proof of Theorem 3: The proof is given in Appendix E.

The unit information energy performance on R for the power amplifier sender is shown in Fig.8. A direct observation is that the curve of unit information energy on the information rate is concave, and there exists appropriate R leading to the minimum unit information energy. At the same time, it is worth noting that in the low R regime, the unit information energy of the HARQ mechanism over different fading channel is almost the same.

Based on the above simulation result and conclusions, we can derive Theorem 4.

Theorem 4: For the OSTBC-MIMO system over Rayleigh and Rician fading channels, there exists an information transmission rate R which leads to the minimum unit information energy $E_b = E_{b\_MIN}$.

Proof of Theorem 4: The proof is given in Appendix E.

V. CONCLUSION AND FUTURE WORK

In this paper, we proposed a LTP-HARQ mechanism to improve the performance of HSTN systems. We synthetically analysis and compare the performance of different retransmission mechanism under the OSTBC-MIMO channels for HSTN system in terms of the mean number of transmission rounds, throughput, file delivery time, and unit information energy, which build a comprehensive performance analysis model for the LTP-HARQ mechanism. Moreover, we discuss the maximum/minimum value problem of the throughput and the unit information energy versus SNR, and give the Theorem 1-4 in different fading cases.

The two main conclusions from our simulation results are: 1) The introduction of lossless HARQ-RR mechanism and multi-antenna system into LTP can greatly reduce the file delivery delay, decrease the energy consumption and enhance the capacity. 2) The minimum-rate or minimum-SNR unit information energy characteristic for lossless HARQ-RR, truncated HARQ-RR and ARQ over the Rician fading channel can be derived in a parameterized semi-closed-form by the Laplace transform approach.

APPENDIX A
DERIVATION OF FORMULA (10)

The energy consumption of the sender that transmits forward frames and receives feedback frames contains: consumption of electronic components of the sender due to pre-transmission processing, energy consumption due to electromagnetic irradiation, energy consumption of electronic components due to the processing of feedback frames, baseband electronic consumption, retransmission statistics and startup energy consumption. The total energy consumption per good-bit can be described as

$$\begin{aligned} E_b &= E_t + E_r \\ &= \varepsilon_{st,tx}\tau_{out} + \varepsilon_{enc} + [(P_{e1,tx} + P_{PA})T_b + P_{e1,rx}T_{fb}]\tau \\ &\quad + \varepsilon_{st,rx}\tau_{out} + [\varepsilon_{dec} + P_{e1,rx}T_b + (P_{e1,tx} + P_{PA})T_{fb}]\tau. \end{aligned} \tag{32}$$

In practice, the startup energy consumption at the sender $\varepsilon_{st,tx}\tau_{out}$ and receiver $\varepsilon_{st,rx}\tau_{out}$ have nothing to do with the calculation for the mean number of transmission rounds and they are ignored in our discussion. Also, the energy required for encoding normalized per data bit and the energy consumption of decoding the forward frame per data bit are related to the number of clock cycles, operating voltage of arithmetic processing unit, the arithmetic operations and other parameters. It is hard to give the accurate calculation and for the convenience we rewrite (32) as follows

$$\begin{aligned} E_b &= [(P_{e1,tx} + P_{PA} + P_{e1,rx})T_b]\tau \\ &\quad + [(P_{e1,rx} + P_{e1,tx} + P_{PA})T_{fb}]\tau + \varepsilon_{dec}\tau. \end{aligned} \tag{33}$$

In the LTP-HARQ mechanism, we set the segment size $L_{seg} = L_{CP} = L_{RS} = N_b$, and we have $T_b = T_{fb}$. T_b is the average time per data nat for pre-transmission processing and actually we have $T_b = D_{seg}/N_b$. The meaning of T_{fb} is similar with T_b, but for the feedback segment or RS in other words. Next, we rewrite it as

$$E_b = A(P_{e1,tx} + P_{PA} + P_{e1,rx})T_b\tau + \varepsilon_{dec}\tau, \tag{34}$$

where A is the coefficient and τ is the the maximum number of successive transmission trials for transmitting one

segment, actually $\tau = M$. $P_{e1,tx}$ is the power consumption of the baseband and radio-frequency electronic components that perform the forward transmission. $P_{e1,rx}$ means the the power consumption at the receiver for feedback segment and it is similar with $P_{e1,tx}$. $P_{e1,tx} + P_{e1,rx} = P_{e1}$ is the total power consumed by the electronic components. P_{PA} is energy consumption due to electromagnetic irradiation and it can be the main energy consumption factor in the long distance HSTN communication scenario.

$$\begin{aligned} E_b &= A(P_{e1} + P_{PA})D_{seg}M/L_{seg} + \varepsilon_{dec}M \\ &= AP_{PA}D_{seg}M/L_{seg} + MAP_{e1}D_{seg}/L_{seg} + \varepsilon_{dec}M \\ &= AP_{PA}D_{seg}M/L_{seg} + ME_{e1} + M\varepsilon_{dec}, \end{aligned} \tag{35}$$

where we use the substitution $\tau = M$, $T_b = D_{seg}/N_b$ and $E_{e1} = AP_{e1}D_{seg}/L_{seg}$. E_{e1} means the unit information energy by the electronic components with band B. We should notice that $P_{PA} = A_1 d^{\alpha} S$, where A_1 is the coefficient corresponding to the power amplifier (PA). d is the distance between the transmitter and receiver and α is the path loss exponent. And it can be rewritten as

$$\begin{aligned} E_b &= A(P_{e1} + P_{PA})D_{seg}M/L_{seg} + ME_{e1} + M\varepsilon_{dec} \\ &= AP_{PA}D_{seg}M/L_{seg} + ME_{e1} + M\varepsilon_{dec} \\ &= AA_1 d^{\alpha} SD_{seg}M/L_{seg} + ME_{e1} + M\varepsilon_{dec} \\ &= A_0 SD_{seg}M/L_{seg} + ME_d, \end{aligned} \tag{36}$$

where we have $A_0 = AA_1 d^{\alpha}$, $E_d = E_{e1} + \varepsilon_{dec}$ and also notice $R = L_{seg}/BD_{seg}$. The normalized-bandwidth information equation for E_b can be rewritten as

$$E_b = \frac{A_0 SR}{MB} + ME_{e1}/B = A_0 \frac{S}{BT} + ME_{dec}, \tag{37}$$

where we have $E_{dec} = E_d/B$. For the convenient of calculation and deration, we set $A_0 = 1$, then we can obtain (10).

APPENDIX B
DERIVATION OF FORMULA (12), (13), (14)

The signal amplitude follows the Rician distribution by [32], which means the non central χ^2 distribution with the degree of freedom of $2N$.

$$p(r) = \frac{r^N}{\sigma^2 \beta^{N-1}} \exp\left(-\frac{\left(r^2 + \beta^2\right)}{2\sigma^2}\right) I_{N-1}\left(\frac{r\beta}{\sigma^2}\right), \tag{38}$$

where non-centrality parameter $\beta = \|\bar{r}\| = \sqrt{\sum_{k=1}^{2N} \bar{r}_k^2} = \sqrt{D^2 N}$ and the shape parameter $K = D^2/2\sigma^2 = D^2$. I_{N-1} is the modified Bessel functions of the first kind with $N-1$ order. Then we can get the distribution of instantaneous power gain $z = r^2$ as follows

$$\begin{aligned} f_z(z) &= \left(\frac{z}{KN}\right)^{(N-1)/2} \exp\left(-\left(z + KN\right)\right) I_{N-1}\left(2\sqrt{KNz}\right) \\ &= \left(\frac{z}{KN}\right)^{(N-1)/2} \exp\left(-\left(z + KN\right)\right) (KNz)^{(N-1)/2} \\ &\quad \times \sum_{i=0}^{\infty} \frac{(KNz)^i}{\Gamma(i+1)\,\Gamma(N+i)} \\ &= z^{N-1} \exp\left(-\left(z + KN\right)\right) \sum_{i=0}^{\infty} \frac{(KNz)^i}{\Gamma(i+1)\,\Gamma(N+i)} \\ &= \sum_{i=0}^{\infty} \frac{(KN)^i z^{N-1+i}}{\Gamma(i+1)\,\Gamma(N+i)} \exp\left(-\left(z + KN\right)\right) \\ &= \sum_{i=0}^{\infty} \frac{\exp(-KN)\,(KN)^i}{\Gamma(i+1)} \frac{z^{N-1+i}\exp(-z)}{\Gamma(N+i)}, \end{aligned} \tag{39}$$

where we can use the series expansion of the modified Bessel functions of the first kind as follows

$$\begin{aligned} I_{N-1}\left(2\sqrt{KNz}\right) &= \left(\sqrt{KNz}\right)^{N-1} \sum_{i=0}^{\infty} \frac{(KNz)^i}{i!\,\Gamma(N-1+i+1)} \\ &= (KNz)^{(N-1)/2} \sum_{i=0}^{\infty} \frac{(KNz)^i}{\Gamma(i+1)\,\Gamma(N+i)}. \end{aligned} \tag{40}$$

Further, the Laplace transform of (39) is

$$F(s) = \sum_{i=0}^{\infty} \frac{e^{-(KN)}(KN)^i}{\Gamma(i+1)} (1+s)^{-(N+i)}. \tag{41}$$

Note that the power series expansion of $e^{-\left(\frac{s}{1+s}KN\right)}$ is

$$e^{-\left(\frac{s}{1+s}KN\right)} = \sum_{i=0}^{\infty} \frac{e^{-(KN)}(KN)^i}{\Gamma(i+1)} (1+s)^{-i}. \tag{42}$$

We can rewrite (41) as follows

$$\begin{aligned} F(s) &= (1+s)^{-N} e^{-\left(\frac{s}{1+s}KN\right)} \\ &= e^{-(KN)} (1+s)^{-N} e^{\left(\frac{KN}{1+s}\right)}. \end{aligned} \tag{43}$$

Combing (5), we have

$$\begin{aligned} Q_k &= \int_0^{\Theta} f_Z{}^{\otimes(k)}(z)dz = \int_0^{\Theta} L^{-1}L\left\{f_Z{}^{\otimes(k)}(z)\right\} dz \\ &= \int_0^{\Theta} L^{-1}F^k(s)dz \\ &= \int_0^{\Theta} L^{-1}\left\{(1+s)^{-kN} e^{\left(\frac{skKN}{1+s}\right)}\right\} dz \\ &= \int_0^{\Theta} L^{-1}\left\{(1+s)^{-kN} \sum_{i=0}^{\infty} \frac{e^{-(kKN)}(kKN)^i}{\Gamma(i+1)} (1+s)^{-i}\right\} dz \\ &= \int_0^{\Theta} L^{-1}\left\{\sum_{i=0}^{\infty} \frac{e^{-(kKN)}(kKN)^i}{\Gamma(i+1)} (1+s)^{-i-kN}\right\} dz. \end{aligned} \tag{44}$$

By the table of Laplace transforms, $L^{-1}\left\{(1+s)^{-i-kN}\right\} = e^{-z} z^{i+kN-1}/\Gamma(i+kN)$, then we have

$$Q_k = \int_0^{\Theta} \left\{\sum_{i=0}^{\infty} \frac{e^{-(kKN)}(kKN)^i}{\Gamma(i+1)} \frac{e^{-z} z^{i+kN-1}}{\Gamma(i+kN)}\right\} dz. \tag{45}$$

We have shown the regularized incomplete gamma function in the previous part of this paper, and at last, we can obtain Q_k as follows

$$Q_k = e^{-(kKN)} \sum_{i=0}^{\infty} \frac{(kKN)^i}{\Gamma(i+1)} \gamma_r(kN+i, \Theta). \tag{46}$$

It is difficult to give the theories proof due to the lack of closed expression about the mean number of transmission rounds over Rician fading. Based on the fact that the Nakagami-m model is generally used to approximate the pdf of the power of a Rician fading signal, we can give the approximate proof. The instantaneous power has pdf over Nakagami-m fading with N order MRC diversity

$$f(z) = \frac{z^{N\alpha-1}}{\beta^{N\alpha}\Gamma(N\alpha)} \exp\left(-\frac{z}{\beta}\right), \tag{47}$$

where $\alpha = m$, $\beta = \frac{\Omega}{m}$. The laplace transform is

$$F(s) = (\beta s + 1)^{-N\alpha}. \tag{48}$$

The mean power value is $\Omega = E(z) = E\left(\|H\|^2\right)$ [33]. And the mean number of transmission rounds is

$$\begin{aligned} M_{nak}^{RR} &= \sum_{k=0}^{\infty} Q_k = \int_0^{\Theta} L^{-1}\left(\frac{1}{1-F(s)}\right)dz \\ &= \int_0^{\Theta} L^{-1}\left(\frac{1}{1-(\beta s+1)^{-N\alpha}}\right)dz \\ &= 1 + \int_0^{\Theta} L^{-1}\left(\frac{1}{(\beta s+1)^{N\alpha}-1}\right)dz \\ &= 1 + \int_0^{\Theta} \exp(-z/\beta)\, L^{-1}\left(\frac{1}{(\beta s)^{N\alpha}-1}\right)dz \\ &= 1 + \int_0^{\Theta} \frac{1}{\beta}\exp(-z/\beta)\, \beta L^{-1}\left(\frac{1}{(\beta s)^{N\alpha}-1}\right)dz. \end{aligned} \tag{49}$$

It is worth noting that the transform $f(at) \Leftrightarrow 1/aF(s/a)$, and we can further rewrite M_{nak}^{RR} as

$$\begin{aligned} &1 + \int_0^{\Theta} \frac{1}{\beta}\exp(-z/\beta) \times \frac{1}{N\alpha}\sum_{j=0}^{N\alpha-1} a_j \exp\left(a_j z/\beta\right)dz \\ &= 1 + \int_0^{\Theta} \frac{1}{\beta}\frac{1}{N\alpha}\sum_{j=0}^{N\alpha-1} a_j \exp\left(\left(a_j-1\right)z/\beta\right)dz \\ &= 1 + \frac{\Theta}{\beta N\alpha} + \int_0^{\Theta} \frac{1}{\beta N\alpha}\sum_{j=1}^{N\alpha-1} a_j \exp\left(\left(a_j-1\right)z/\beta\right)dz \\ &= 1 + \frac{\Theta}{\beta N\alpha} + \frac{1}{N\alpha}\sum_{j=1}^{N\alpha-1} \frac{1}{\left(1-a_j{}^*\right)} \exp\left(-\left(1-a_j\right)\Theta/\beta\right) \\ &\quad - \frac{1}{N\alpha}\sum_{j=1}^{N\alpha-1} \frac{1}{\left(1-a_j{}^*\right)}. \end{aligned} \tag{50}$$

Further, we have

$$\begin{aligned} M_{nak}^{RR} &= 1 + \frac{\Theta}{\beta N\alpha} \\ &\quad + \frac{1}{N\alpha}\sum_{j=1}^{N\alpha-1} \frac{\exp\left(-\Theta\left(1-a_j\right)/\beta\right)}{\left(1-a_j{}^*\right)} - \frac{1}{N\alpha}\frac{N\alpha-1}{2} \\ &= \frac{N\alpha+1}{2N\alpha} + \frac{\Theta}{\beta N\alpha} + \frac{1}{N\alpha}\sum_{j=1}^{N\alpha-1} \frac{\exp\left(-\Theta\left(1-a_j\right)/\beta\right)}{\left(1-a_j{}^*\right)} \\ &= \frac{Nm+1}{2Nm} + \frac{\Theta}{N\Omega} + \frac{1}{Nm}\sum_{j=1}^{Nm-1} \frac{\exp\left(-\Theta\left(1-a_j\right)\frac{m}{\Omega}\right)}{\left(1-a_j{}^*\right)}, \end{aligned} \tag{51}$$

where $a_j{}^* = \exp(-i2\pi j/N\alpha)$. For the different value of Ω and m, the Nakagami-m fading can be seen as Rayleigh or Rician fading. For example, the Nakagami-m fading generates to the Rayleigh fading with N order diversity by setting $m = 1$. By setting $m = \frac{K^2+2K+1}{2K+1}$, we can view the Nakagami-m model as the approximation of the Rician model.

APPENDIX C
PROOF OF THEOREM 1

Assuming $\Theta = (e^{R/r} - 1)/\widetilde{S}$, $\widetilde{S} = S/rN_t$, $N_t = m$. Set $\Theta = h/S$, $h = rN_t(e^{R/r} - 1)$, and we have the limit of unit information energy by making SNR sufficiently close to 0 or infinity

$$\begin{aligned} \lim_{S\to 0} E_b &= \lim_{S\to 0}\left\{\frac{SM_{nak}^{RR}}{BR} + M_{nak}^{RR}E_{dec}^{RR}\right\} \\ &= \lim_{S\to 0}\left\{\frac{S\left\{\frac{\Theta}{N\Omega}\right\}}{BR} + M_{nak}^{RR}E_{dec}\right\} \\ &= \lim_{S\to 0}\left\{\frac{h}{BN\Omega R} + \infty\right\} = \infty, \end{aligned} \tag{52}$$

and

$$\begin{aligned} \lim_{S\to\infty} E_b &= \lim_{S\to\infty}\left\{\frac{SM_{nak}^{RR}}{BR} + M_{nak}^{RR}E_{dec}^{RR}\right\} \\ &= \lim_{S\to\infty}\left\{\frac{S\{\infty\}}{BR} + M_{nak}^{RR}E_{dec}\right\} \\ &= \lim_{S\to 0}\{\infty + E_{dec}\} = \infty. \end{aligned} \tag{53}$$

According to the maximum value theorem of the continuous function on an open interval, there exists minimum value of E_b on interval $(0, \infty)$. Moreover, when $S \to 0$, the energy consumption of the transmitter is limited to the constant $\frac{rN_t(e^{R/r}-1)}{BN\Omega R}$. Thus, without considering the energy consumption of the receiver, the infinite retransmission rounds can promise the successful decoding.

APPENDIX D
PROOF OF THEOREM 2

Consider the truncated HARQ over Nakagami-m fading and if $S \to 0 \Leftrightarrow \Theta \to \infty$, we have

$$\begin{aligned}\lim_{S\to 0} E_b &= \lim_{S\to 0}\left\{\frac{SM_{nak}^C}{BR} + M_{nak}^C E_{dec}^C\right\}\\ &= \lim_{\Theta\to\infty}\left\{\frac{h\left\{1+\sum_{k=1}^{C-1}\gamma_r\left(km, \frac{m}{\Omega}\Theta\right)\right\}}{\Theta BR\Gamma_r\left(mC, \frac{m}{\Omega}\Theta\right)} + M_{nak}^C E_{dec}\right\}\\ &= \lim_{S\to 0}\left\{\infty + M_{nak}^{RR} E_{dec}\right\} = \infty, \end{aligned} \tag{54}$$

where the key of (54) is

$$\begin{aligned}&\lim_{\Theta\to\infty}\Theta\Gamma_r\left(mC, \frac{m}{\Omega}\Theta\right)\\ &= \lim_{\Theta\to\infty}\frac{\Gamma_r\left(mC, \frac{m}{\Omega}\Theta\right)}{1/\Theta}\\ &= \lim_{\Theta\to\infty}\left\{\frac{-\frac{1}{\Gamma(mC)}\Theta^{mC-1}e^{-m\Theta/\Omega}}{-1/\Theta^2}\right\}\\ &= \lim_{\Theta\to\infty}\left\{\frac{1}{\Gamma(mC)}\Theta^{mC+1}e^{-m\Theta/\Omega}\right\} = 0, \end{aligned} \tag{55}$$

and we have

$$\lim_{S\to 0} E_b = \lim_{\Theta\to\infty}\left\{\infty + M_{Ray}^C E_{dec}^C\right\} = \infty. \tag{56}$$

For the case of $S \to \infty$, the bound of the unit information energy is

$$\begin{aligned}\lim_{\Theta\to 0} E_b &= \lim_{\Theta\to 0}\left\{\frac{S}{BT_{Nak}^C} + M_{Nak}^C E_{dec}^C\right\}\\ &= \lim_{\Theta\to 0}\left\{\frac{h\left\{1+\sum_{k=1}^{C-1}\gamma_r(km, \frac{m}{\Omega}\Theta)\right\}}{\Theta BR\Gamma_r(mC, \frac{m}{\Omega}\Theta)} + M_{Nak}^C E_{dec}^C\right\}\\ &= \lim_{\Theta\to\infty}\left\{\infty + E_{dec}^C\right\}. \end{aligned} \tag{57}$$

We can set truncated HARQ $C = 1$, then we have the same demonstration for ARQ. Both the retransmission mechanism, truncated HARQ and ARQ, can not completely promise the successful decoding.

APPENDIX E
PROOF OF THEOREM 3 AND THEOREM 4

Assuming $rN_t(e^{R/r}-1) = \Theta\times S, R = r\ln\left(\frac{\Theta S}{rN_t}+1\right)$, if $R \to 0 \Leftrightarrow \Theta \to 0$, the bound of throughput is

$$\begin{aligned}\lim_{R\to 0} T_{Nak}^{RR} &= \lim_{\Theta\to 0}\left\{\frac{r\ln\left(\frac{\Theta S}{rm}+1\right)}{\frac{m+1}{2m} + \frac{\Theta}{\Omega} + \frac{1}{m}\sum_{j=1}^{m-1}\frac{\exp\left(-\frac{m}{\Omega}\Theta(1-a_j)\right)}{(1-a_j^*)}}\right\}\\ &= 0, \end{aligned} \tag{58}$$

if $R \to \infty$, we can obtain

$$\begin{aligned}\lim_{R\to\infty} T_{Nak}^{RR} &= \lim_{\Theta\to\infty}\left\{\frac{r\ln\left(\frac{\Theta S}{rm}+1\right)}{\frac{m+1}{2m} + \frac{\Theta}{\Omega} + \frac{1}{m}\sum_{j=1}^{m-1}\frac{\exp\left(-\frac{m}{\Omega}\Theta(1-a_j)\right)}{(1-a_j^*)}}\right\}\\ &= \lim_{\Theta\to\infty}\left\{\frac{r\ln\left(\frac{\Theta S}{rm}+1\right)}{\frac{\Theta}{\Omega}}\right\} = \lim_{\Theta\to\infty}\left\{\frac{r\Omega}{\frac{\Theta S}{rm}+1}\right\}\\ &= 0. \end{aligned} \tag{59}$$

On the one hand, from (58) and (59), we can see that there exists a R leads to the maximum throughput. On the other hand, according to the property of function and combing the definition (10) and (6), there exists a R leads to the minimum unit information energy. The proof of theorem 3 and theorem 4 are finished.

ACKNOWLEDGMENT

Jian Jiao, Youjun Hu, and Qinyu Zhang contributed equally to this work.

REFERENCES

[1] M. X. Jia Gu, Q. Guo, W. Xiang, and N. Zhang, "Broadband hybrid satellite-terrestrial communication systems based on cognitive radio toward 5G," *IEEE Wireless Commun.*, vol. 23, no. 6, pp. 96–106, Dec. 2016.

[2] Q. Y. Yu, W. X. Meng, M. C. Yang, and L. M. Zheng, "Virtual multi-beamforming for distributed satellite clusters in space information networks," *IEEE Wireless Commun.*, vol. 23, no. 1, pp. 95–101, Feb. 2016.

[3] S. Burleigh, M. Ramadas, and S. Farrell, *Licklider Transmission Protocol—Motivation*, document RFC 5325, 2008. [Online]. Available: https://www.rfc-editor.org/rfc/pdfrfc/rfc5325.txt.pdf

[4] M. Ramadas, S. Burleigh, and S. Farrell, *Licklider Transmission Protocol—Specification*, document RFC 5326, 2008. [Online]. Available: https://www.rfc-editor.org/rfc/pdfrfc/rfc5326.txt.pdf

[5] J. Jiao, X. Sui, S. Gu, S. Wu, and Q. Zhang, "Partially observable Markov decision process-based transmission policy over Ka-band channels for space information networks," *Entropy*, vol. 63, no. 9, p. 510, 2017.

[6] P. D. Arapoglou, K. Liolis, M. Bertinelli, A. Panagopoulos, P. Cottis, and R. Gaudenzi, "MIMO over satellite: A review," *IEEE Commun. Surveys Tuts.*, vol. 13, no. 1, pp. 27–51, 1st Quart., 2011.

[7] P. Larsson, L. K. Rasmussen, and M. Skoglund, "Throughput analysis of ARQ schemes in Gaussian block fading channels," *IEEE Trans. Commun.*, vol. 62, no. 7, pp. 2569–2588, Jul. 2014.

[8] Q. Yu, R. Wang, Z. Wei, X. Sun, and J. Hou, "DTN Licklider transmission protocol over asymmetric space channels," *IEEE Aerosp. Electron. Syst. Mag.*, vol. 28, no. 5, pp. 14–22, May 2013.

[9] R. Wang, S. C. Burleigh, P. Parikh, C. J. Lin, and B. Sun, "Licklider transmission protocol (LTP)-based DTN for cislunar communications," *IEEE/ACM Trans. Netw.*, vol. 19, no. 2, pp. 359–368, Feb. 2011.

[10] Q. Yu, S. C. Burleigh, R. Wang, and K. Zhao, "Performance modeling of Licklider transmission protocol (LTP) in deep-space communication," *IEEE Trans. Aerosp. Electron. Syst.*, vol. 51, no. 3, pp. 1609–1620, Jul. 2015.

[11] K. Zhao, R. Wang, S. C. Burleigh, M. Qiu, A. Sabbagh, and J. Hu, "Modeling memory-variation dynamics for the Licklider transmission protocol in deep-space communications," *IEEE Trans. Aerosp. Electron. Syst.*, vol. 51, no. 4, pp. 2510–2524, Oct. 2015.

[12] L. Clare and G. Miles, "Deep space optical link ARQ performance analysis," in *Proc. IEEE Aerosp. Conf.*, Big Sky, MT, USA, Mar. 2016, pp. 1–11.

[13] I. Bettesh and S. S. Shamai, "Optimal power and rate control for minimal average delay: The single-user case," *IEEE Trans. Inf. Theory*, vol. 52, no. 9, pp. 4115–4141, Sep. 2006.
[14] C. Shen, T. Liu, and M. P. Fitz, "Aggressive transmission with ARQ in quasi-static fading channels," in *Proc. IEEE Int. Conf. Commun.*, Beijing, China, May 2008, pp. 1092–1097.
[15] P. Larsson, B. Smida, T. Koike-Akino, and V. Tarokh, "Analysis of network coded HARQ for multiple unicast flows," *IEEE Trans. Commun.*, vol. 61, no. 2, pp. 722–732, Feb. 2013.
[16] J. Kim, H. Jin, D. K. Sung, and R. Schober, "Optimal rate allocation for wireless multicast systems employing hybrid-ARQ with chase combining," in *Proc. IEEE 21st Annu. IEEE Int. Symp. Pers. Indoor Mobile Radio Commun.*, Instanbul, Turkey, Sep. 2010, pp. 1207–1211.
[17] L. Szczecinski, S. R. Khosravirad, P. Duhamel, and M. Rahman, "Rate allocation and adaptation for incremental redundancy truncated HARQ," *IEEE Trans. Commun.*, vol. 61, no. 6, pp. 2580–2590, Jun. 2013.
[18] M. Jabi, L. Szczecinski, M. Benjillali, and F. Labeau, "Outage-optimal power adaptation and allocation for truncated HARQ," in *Proc. IEEE Int. Conf. Commun.*, Sydney, NSW, Australia, Jun. 2014, pp. 1890–1896.
[19] P. Larsson, L. K. Rasmussen, and M. Skoglund, "Throughput analysis of hybrid-ARQ: A matrix exponential distribution approach," *IEEE Trans. Commun.*, vol. 64, no. 1, pp. 416–428, Jan. 2016.
[20] I. Stanojev, O. Simeone, Y. Bar-Ness, and D. H. Kim, "Energy efficiency of non-collaborative and collaborative hybrid-ARQ protocols," *IEEE Trans. Wireless Commun.*, vol. 8, no. 1, pp. 326–335, Jan. 2009.
[21] F. Rosas *et al.*, "Optimizing the code rate of energy-constrained wireless communications with HARQ," *IEEE Trans. Wireless Commun.*, vol. 15, no. 1, pp. 191–205, Jan. 2016.
[22] M. Jabi, M. Benjillali, and F. Labeau, "Energy efficiency of adaptive HARQ," *IEEE Trans. Commun.*, vol. 61, no. 2, pp. 818–831, Feb. 2016.
[23] S. Ge, Y. Xi, H. Zhao, S. Huang, and J. Wei, "Energy efficient optimization for CC-HARQ over block Rayleigh fading channels," *IEEE Commun. Lett.*, vol. 19, no. 10, pp. 1854–1857, Oct. 2015.
[24] Y. Wu and H. Yang, "Optimising energy efficiency of LDPC coded chase combining HARQ system," *Electron. Lett.*, vol. 51, no. 6, pp. 490–492, Mar. 2015.
[25] L. Shi *et al.*, "Integration of Reed–Solomon codes to Licklider transmission protocol (LTP) for space DTN," *IEEE Aerosp. Electron. Syst. Mag.*, vol. 32, no. 4, pp. 48–55, Apr. 2017.
[26] C. Berrou, A. Glavieux, and P. Thitimajshima, "Near Shannon limit error-correcting coding and decoding: Turbo-codes," in *Proc. IEEE Int. Conf. Commun.*, Geneva, Switzerland, May 1993, pp. 1064–1070.
[27] G. Wang, H. Shen, Y. Sun, J. R. Cavallaro, A. Vosoughi, and Y. Guo, "Parallel interleaver design for a high throughput HSPA+/LTE multi-standard turbo decoder," *IEEE Trans. Circuits Syst. I, Reg. Papers*, vol. 61, no. 5, pp. 1376–1389, May 2014.
[28] Y. S. Park, D. Blaauw, D. Sylvester, and Z. Zhang, "Low-power high-throughput LDPC decoder using non-refresh embedded DRAM," *IEEE J. Solid-State Circuits*, vol. 49, no. 3, pp. 783–794, Mar. 2014.
[29] H. Wu, Q. Zhang, Z. Yang, J. Jiao, Y. Li, and S. Gu, "Double retransmission deferred negative acknowledgement in consultative committee for space data systems file delivery protocol for space communications," *IET Commun.*, vol. 10, no. 3, pp. 245–252, Mar. 2016.
[30] G. Caire and D. Tuninetti, "The throughput of hybrid-ARQ protocols for the Gaussian collision channel," *IEEE Trans. Inf. Theory*, vol. 47, no. 5, pp. 1971–1988, Jul. 2001.
[31] E. Larsson, P. Stoica, and G. Ganesan, *Space-Time Block Coding for Wireless Communications*. Cambridge, U.K.: Cambridge Univ. Press, 2003.
[32] M. K. Simon, *Probability Distributions Involving Gaussian Random Variables*. Boston, MA, USA: Springer, 2006.
[33] N. Kumar, P. K. Singya, and V. Bhatia, "Performance analysis of orthogonal frequency division multiplexing-based cooperative amplify-and-forward networks with non-linear power amplifier over independently but not necessarily identically distributed Nakagami-*m* fading channels," *IET Commun.*, vol. 11, no. 7, pp. 1008–1020, Jul. 2017.

JIAN JIAO (M'16) received the M.S. and Ph.D. degrees in communication engineering from the Harbin Institute of Technology (HIT), in 2007 and 2011, respectively. From 2011 to 2015, he was a Post-Doctoral Research Fellow with the Communication Engineering Research Centre, Shenzhen Graduate School, HIT, Shenzhen, China. From 2016 to 2017, he was a China Scholarship Council Visiting Scholar with the School of Electrical and Information Engineering, University of Sydney, Sydney, Australia. Since 2017, he has been an Assistant Professor with the Department of Electrical and Information Engineering, HIT Shenzhen Graduate School. He has authored or co-authored over 60 peer-reviewed papers, holds over 30 invention patents in his research fields. His current interests include error control codes, space information networks, random multiple access, and machine-to-machine communications. He received the Shenzhen High Level Talent Program Award in 2015.

YOUJUN HU received the bachelor's degree in communication engineering from the Harbin Institute of Technology, Harbin, in 2015. He is currently pursuing the master's degree with the Communication Engineering Research Centre, School of Electrical and Information Engineering, Harbin Institute of Technology Shenzhen, China. His research interests include space information networks, error control codes, and machine-to-machine communications.

QINYU ZHANG (M'08–SM'12) received the bachelor's degree in communication engineering from the Harbin Institute of Technology (HIT) in 1994, and the Ph.D. degree in biomedical and electrical engineering from the University of Tokushima, Japan, in 2003. From 1999 to 2003, he was an Assistant Professor with the University of Tokushima. From 2003 to 2005, he was an Associate Professor with the Shenzhen Graduate School, HIT, and the Founding Director with the Communication Engineering Research Centre, School of Electronic and Information Engineering. Since 2005, he has been a Full Professor, and serves as the Dean with the EIE School. His research interests include aerospace communications and networks, wireless communications and networks, cognitive radios, signal processing, and biomedical engineering. He was a TPC Member for the INFOCOM, the ICC, the GLOBECOM, the WCNC, and other flagship conferences in communications. He received the National Science Fund for Distinguished Young Scholars, the Young and Middle-Aged Leading Scientist of China, the Chinese New Century Excellent Talents in University, and received three scientific and technological awards from governments. He was the TPC Co-Chair of the IEEE/CIC ICCC'15, the Symposium Co-Chair of the IEEE VTC'16 Spring, an Associate Chair for Finance of ICMMT'12, and the Symposium Co-Chair of CHINACOM'11. He was the Founding Chair of the IEEE Communications Society Shenzhen Chapter. He is on the Editorial Board of some academic journals, such as, the *Journal on Communications*, *KSII Transactions on Internet and Information Systems*, and *Science China: Information Sciences.*

SHAOHUA WU (S'07–M'11) received the Ph.D. degree in communication engineering from the Harbin Institute of Technology in 2009. From 2009 to 2011, he was a Post-Doctoral Researcher with the Department of Electronics and Information Engineering, Shenzhen Graduate School of Harbin Institute of Technology (HITSZS). He has been an Associate Professor with HITSZS, since 2012. His current research interests include wireless image/video transmission, deep space communication, IR-UWB ranging/localization/communication, and 5G wireless transmission technologies.